

# Top-Quark Decay at Next-to-Next-to-Leading Order in QCD

Jun Gao,<sup>1,\*</sup> Chong Sheng Li,<sup>2,3,†</sup> and Hua Xing Zhu<sup>4,‡</sup>

<sup>1</sup>*Department of Physics, Southern Methodist University, Dallas, Texas 75275-0175, USA*

<sup>2</sup>*Department of Physics and State Key Laboratory of Nuclear Physics and Technology, Peking University, Beijing 100871, China*

<sup>3</sup>*Center for High Energy Physics, Peking University, Beijing 100871, China*

<sup>4</sup>*SLAC National Accelerator Laboratory, Stanford University, Stanford, California 94309, USA*

(Received 13 October 2012; published 24 January 2013)

We present the complete calculation of the top-quark decay width at next-to-next-to-leading order in QCD, including next-to-leading electroweak corrections as well as finite bottom quark mass and  $W$  boson width effects. In particular, we also show the first results of the fully differential decay rates for the top-quark semileptonic decay  $t \rightarrow W^+(l^+ \nu)b$  at next-to-next-to-leading order in QCD. Our method is based on the understanding of the invariant mass distribution of the final-state jet in the singular limit from effective field theory. Our result can be used to study arbitrary infrared-safe observables of top-quark decay with the highest perturbative accuracy.

DOI: [10.1103/PhysRevLett.110.042001](https://doi.org/10.1103/PhysRevLett.110.042001)

PACS numbers: 12.38.Bx, 14.65.Ha

**Introduction.**—The top quark is the heaviest fermion in the standard model (SM), and frequently plays an important role in many extensions of the SM. Therefore, detailed studies of its production and decay are highly desirable. Their precise measurements at the LHC will be crucial for the understanding of electroweak symmetry breaking and also searching for new physics. Due to its large mass, the lifetime of the top quark is much smaller than the typical time scale of hadronization. For this reason, the top quark can be treated as a free particle in good approximation, and perturbative calculations of higher order quantum corrections to its decay rate can be performed.

Within the SM, the next-to-leading order (NLO) quantum chromodynamics (QCD) corrections to the top-quark decay width,  $\Gamma_t$ , were calculated more than 20 years ago [1]. Employing the method developed in Ref. [2], the next-to-next-to-leading order (NNLO) QCD corrections to  $\Gamma_t$  were calculated in Ref. [3], in the limit of  $m_t \gg m_W$ . Later, the finite  $W$  boson mass effect in the NNLO computation was taken into account in Refs. [4,5] based on the calculations of top-quark self-energy as an expansion in  $m_W^2/m_t^2$ . All the previous calculations at NNLO concentrate only on the inclusive decay width, but the differential decay rate is also of substantial interest, especially when considering the measurement of top-quark mass [6] and electroweak (EW) couplings [7]. In particular, it is an important ingredient in a fully differential calculation of top-quark pair production [8] and decay at NNLO in QCD. To the best of our knowledge, such a calculation has not been finished so far and is the subject of this Letter, in addition to the total decay width of the top quark.

**The formalism.**—We consider the SM top-quark decay,

$$t \rightarrow W^+ + b + X, \quad (1)$$

where  $X$  represents any other parton in the final state. NNLO QCD corrections to this process consists of three

parts: two-loop virtual contribution ( $X$  contains nothing), one-loop real-virtual contribution ( $X$  contains 1 parton), and tree-level double real contribution ( $X$  contains 2 partons). While the amplitudes for each part are well defined, integrals over the phase space induce infrared singularities, which must be extracted to cancel against those from virtual corrections in order to obtain a finite result. In particular, the double real contribution is the primary obstacle for obtaining fully differential NNLO corrections. In the past decade significant efforts have been devoted to solving this problem, and fully differential corrections have been obtained for a number of important processes using quite different methods [8–10]. In this Letter, we solve this problem for processes of heavy-to-light decay at NNLO in QCD, using a phase space slicing method inspired by a factorization formula for heavy-to-light current in the soft-collinear effective theory (SCET) [11]. Below we describe our method.

To begin with, we set bottom quark mass  $m_b = 0$  in the NLO and NNLO QCD calculations. Effects of finite  $m_b$  are small and will be considered later as a correction to the leading order (LO) results. We cluster all the partons in the final state into a single jet, letting  $\tau = (p_b + p_X)^2/m_t^2$ , which measures the invariant mass of the jet. In the limit of  $\tau \rightarrow 0$ , only soft radiations and (or) radiations collinear to the  $b$  quark are allowed. In this region,  $\frac{d\Gamma_t}{d\tau}$  obeys a factorization formula [12]:

$$\begin{aligned} \frac{1}{\Gamma_t^{(0)}} \frac{d\Gamma_t}{d\tau} &= \mathcal{H}\left(x \equiv \frac{m_W^2}{m_t^2}, \mu\right) \int dk dm^2 J(m^2, \mu) S(k, \mu) \\ &\times \delta\left(\tau - \frac{m^2 + 2E_J k}{m_t^2}\right) + \dots, \end{aligned} \quad (2)$$

where we have neglected nonsingular terms in  $\tau$ .  $\Gamma_t^{(0)}$  is the top-quark decay width at LO,  $\mu$  is the renormalization scale, and  $E_J = (m_t^2 - m_W^2)/(2m_t)$  is the energy of the

jet near threshold.  $\mathcal{H}(x, \mu)$  is the hard function, which results from integrating out hard modes of QCD in matching to SCET. It has been calculated to NNLO in  $\alpha_s$  [13].  $J(m^2, \mu)$  is the quark jet function with mass  $m$ , whose NNLO expression can be found in Ref. [14]. It can be thought of as the probability of finding a jet with invariant mass  $m$ , generated by collinear radiations.  $S(k, \mu)$  is the soft function, which describes the probability of measuring the light-cone component of the momentum of soft radiations  $k_s \cdot n$ , where  $n$  is a unit light-cone vector along the direction of the jet, to be  $k$ . It has also been calculated to NNLO in Ref. [15].

Furthermore, the top-quark decay width  $\Gamma_t$  can be divided into two parts:

$$\Gamma_t = \int_0^{\tau_0} d\tau \frac{d\Gamma_t}{d\tau} + \int_{\tau_0}^{\tau_{\max}} d\tau \frac{d\Gamma_t}{d\tau} \equiv \Gamma_A + \Gamma_B, \quad (3)$$

which will be treated separately as explained below.  $\tau_0$  is a dimensionless cutoff for  $\tau$ , and  $\tau_{\max} = (1 - m_W/m_t)^2$ . First, using the NNLO results for the hard function, jet function, and soft function, we can calculate  $\Gamma_A$  at NNLO, utilizing Eq. (2), up to terms proportional to  $\tau_0$ . For sufficiently small  $\tau_0$ , they can be safely neglected. The most difficult part of the double real contributions are included in the calculations of the jet function and soft function. Note that  $\Gamma_A$  is infrared finite, because the infrared divergences in the jet and soft function cancel against those from the hard function. The spin information of the  $b$  quark is lost because spin summation has been performed in the jet function. But polarization information of the top quark is retained, due to the fact that soft radiations do not change spin. In practice, instead of a convolution form, it's more convenient to write Eq. (2) in a product form:

$$\frac{1}{\Gamma_t^{(0)}} \frac{d\Gamma_t}{d\tau} = \mathcal{H}(x, \mu) \lim_{\eta \rightarrow 0} \tilde{j}\left(\partial_\eta + \ln \frac{m_t^2}{\mu^2}, \mu\right) \times \tilde{s}\left(\partial_\eta + \ln \frac{m_t^2}{2E_J \mu}, \mu\right) \frac{\tau^\eta}{\tau} \frac{e^{-\gamma_E \eta}}{\Gamma(\eta)}, \quad (4)$$

where  $\tilde{j}$  and  $\tilde{s}$  are the Laplace trasformed jet and soft function, respectively:

$$\begin{aligned} \tilde{j}\left(\ln \frac{\nu m_t^2}{\mu^2}, \mu\right) &= \int_0^\infty dm^2 \exp\left(-\frac{\nu m^2}{e^{\gamma_E} m_t^2}\right) J(m^2, \mu), \\ \tilde{s}\left(\ln \frac{\nu m_t^2}{2E_J \mu}, \mu\right) &= \int_0^\infty dk \exp\left(-\frac{2\nu E_J k}{e^{\gamma_E} m_t^2}\right) S(k, \mu), \end{aligned} \quad (5)$$

and  $\tau^\eta/\tau$  should be expanded in terms of plus distribution:

$$\frac{\tau^\eta}{\tau} = \frac{1}{\eta} \delta(\tau) + \sum_{n=0}^\infty \frac{\eta^n}{n!} \left[ \frac{\ln^n \tau}{\tau} \right]_+. \quad (6)$$

Substituting the NNLO expansion for the hard function, jet function, and soft function into Eq. (4) gives a closed form solution of  $d\Gamma_t/d\tau$  at small  $\tau$ .

$\Gamma_B$  is also infrared finite. In fact,  $\mathcal{O}(\alpha_s^2)$  contribution to it can be obtained from the NLO QCD corrections to  $t \rightarrow W^+ b$  plus 1 jet, as long as  $\tau_0 > 0$ . In our calculation, the one-loop helicity amplitudes for this specific process are extracted from the NLO QCD corrections to the single top production associated with the  $W$  boson [16]. The tree-level helicity amplitudes are calculated with helicity amplitudes subroutines [17]. Infrared divergences in the phase space integral of tree-level matrix elements are canceled by adding appropriate dipole subtraction terms [18]. For later convenience, we further divided the  $\mathcal{O}(\alpha_s^2)$  contributions from  $\Gamma_B$  into two pieces: tree-level  $t \rightarrow W^+ b + 2$  jets plus dipole subtraction terms  $\Gamma_3^{(2)}$ , and one-loop  $t \rightarrow W^+ b + 1$  jet plus integrated dipole terms  $\Gamma_2^{(2)}$ . Together with the NNLO corrections to  $\Gamma_A$ , denoted by  $\Gamma_1^{(2)}$ , they add up to the full NNLO QCD corrections to  $\Gamma_t$ .

Finally, we note that throughout the calculation in this Letter, the strong coupling constant is renormalized in the modified  $\overline{\text{MS}}$  scheme [19], and renormalization of masses, wave functions, and the electroweak coupling constant are carried out in the on-shell scheme [20]. It should be pointed out that the method used here to calculate the NNLO corrections is similar to the  $q_T$  subtraction method of Catani and Grazzini [10]. In fact, they both employ the universality of infrared divergences and the knowledge of resummation to facilitate the calculation.

**Total width.**—For top-quark SM decay, the total decay width in the  $G_F$  parametrization scheme [20] at LO is given by

$$\Gamma_t^{(0)} = \frac{G_F m_t^3}{8\sqrt{2}\pi} \left[ 1 - 3\left(\frac{m_W^2}{m_t^2}\right)^2 + 2\left(\frac{m_W^2}{m_t^2}\right)^3 \right],$$

assuming a Cabibbo-Kobayashi-Maskawa matrix element  $|V_{tb}| = 1$  and  $m_b = 0$ . We choose  $m_W = 80.385$  GeV,  $G_F = 1.16638 \times 10^{-5}$  GeV $^{-2}$ , and  $m_t = 173.5$  GeV [21], unless specified. Other constants used in followed calculations include  $m_Z$ ,  $\alpha_s(m_Z)$ , and  $m_b$ , which are also chosen as in Ref. [21]. Corrections to the LO width considered here include finite  $b$  quark mass and  $W$  boson width effects,  $\delta_f^b$  and  $\delta_f^W$ , NLO electroweak corrections,  $\delta_{\text{EW}}$ , NLO and NNLO QCD corrections,  $\delta_{\text{QCD}}^{(1)}$  and  $\delta_{\text{QCD}}^{(2)}$ , which are defined as

TABLE I. Top-quark total width at LO and corrections in percentage (%) from finite  $W$  boson width, finite  $b$  quark mass, and high orders, including NLO in EW couplings and NLO and NNLO in QCD coupling. Mass and width are shown in unit of GeV.

$m_t$	$\Gamma_t^{(0)}$	$\delta_f^b$	$\delta_f^W$	$\delta_{\text{EW}}$	$\delta_{\text{QCD}}^{(1)}$	$\delta_{\text{QCD}}^{(2)}$
172.5	1.4806	-0.26	-1.49	1.68	-8.58	-2.09
173.5	1.5109	-0.26	-1.49	1.69	-8.58	-2.09
174.5	1.5415	-0.25	-1.48	1.69	-8.58	-2.09

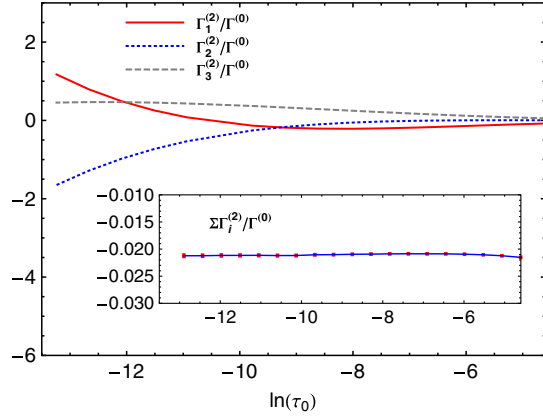


FIG. 1 (color online). Separate contributions of the NNLO QCD corrections and their sum as functions of the cutoff  $\tau_0$ , normalized to the LO width.

$$\Gamma_t = \Gamma_t^{(0)}(1 + \delta_f^b + \delta_f^W + \delta_{EW} + \delta_{QCD}^{(1)} + \delta_{QCD}^{(2)}),$$

where  $\Gamma_t$  is the corrected total width. In Table I we show the LO total width together with all the corrections in percentage (%) for different top-quark mass values. The renormalization scale is set to top-quark mass. Our results agree with those shown in previous literature for finite width and mass effects [1], electroweak corrections [20,22], and NLO QCD corrections [1] with the updated input parameters. Especially, although using quite different method, our NNLO QCD corrections agree with the results in Ref. [5] within the range of the uncertainties of numerical calculation, which are of the order  $10^{-4}$ . All the corrections are stable with respect to the top-quark mass.

As mentioned earlier, the NNLO QCD corrections can be divided into three pieces,  $\Gamma_i^{(2)}$  with  $i = 1, 2, 3$ . Each depends strongly on the cutoff parameter  $\tau_0$  up to the fourth power of  $\ln\tau_0$ . While their sum should only have weak dependencies proportional to  $\tau_0$ , they approach the genuine NNLO QCD corrections when  $\tau_0$  is small enough.

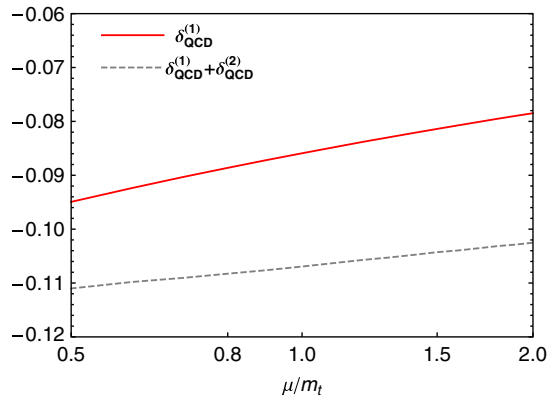


FIG. 2 (color online). Renormalization scale dependence of the NLO and NLO + NNLO QCD corrections, normalized to the LO width at central scale  $\mu = m_t$ .

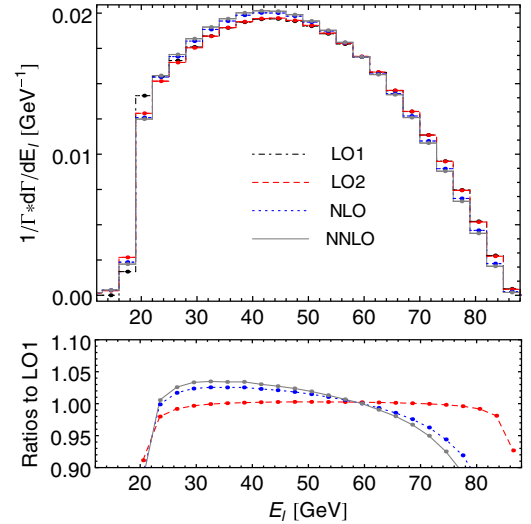


FIG. 3 (color online). Energy distribution of the charged lepton from top-quark decay in the top-quark rest frame.

Thus in Fig. 1 we show the separate contributions to the NNLO corrections. When  $\tau_0$  varies from  $10^{-3}$  to about  $10^{-6}$ , the separate contributions can reach as large as twice the LO width, while the sum remains almost unchanged at the value of about 2.1% of the LO width. Stability of such a large cancellation proves the validity of our NNLO calculation. On the other hand, the NLO QCD corrections have an uncertainty of about 1.6% of the LO width due to the arbitrary choice of renormalization scale as shown in Fig. 2, which comes directly from running the QCD coupling constant  $\alpha_s$ . After adding the NNLO QCD corrections, the scale dependence is reduced to about 0.8%, which makes the predictions more reliable.

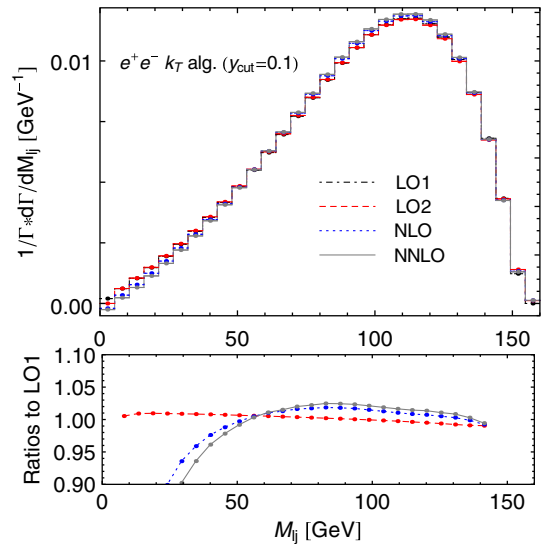


FIG. 4 (color online). Invariant mass distribution of the charged lepton and the hardest jet from top-quark decay in the top-quark rest frame.

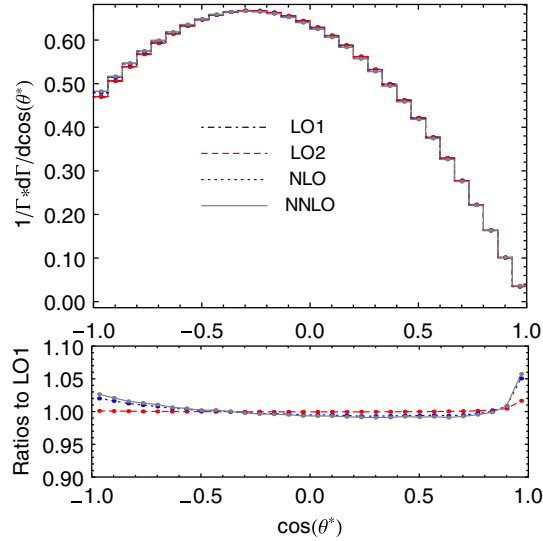


FIG. 5 (color online). Angular distribution of the charged lepton from top-quark decay in the  $W$  boson rest frame.

*Differential distributions.*—Within our framework we can calculate the fully differential decay width of top-quark semileptonic decay  $t \rightarrow W^+(l^+ \nu)b$  up to NNLO in QCD, which is not possible for the method based on calculations of top-quark self-energy. Precise predictions for differential distributions of top-quark decay products are of great importance, especially for the measurement of top-quark mass [6] and testing of the  $V-A$  structure of the  $tWb$  charged current [7]. Below we will show several final-state distributions for  $t \rightarrow W^+(l^+ \nu)b$ , including all the corrections as in the total width results. We use  $e^+e^- k_T$  algorithm [23] at the parton level with jet resolution threshold  $y_{\text{cut}} = 0.1$  for jet clustering, which is more suitable for presentation of the results in top-quark rest frame as compared to the jet algorithms used at the LHC. The shape

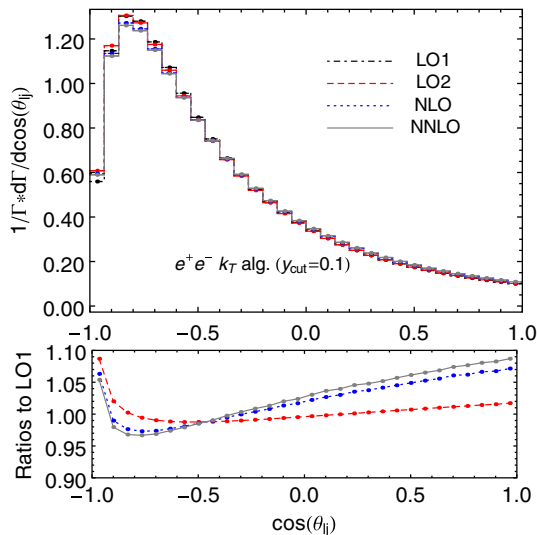


FIG. 6 (color online). Angular distribution of the charged lepton from top-quark decay in the top-quark rest frame.

measurements are more relevant for the experimental studies, having both small experimental and theoretical uncertainties. Thus all the distributions shown below are normalized to unit area for comparison. For each distribution we show results for several cases, i.e., pure LO prediction (denoted by LO1), LO predictions plus corrections from finite  $m_b$ ,  $W$  boson width and NLO EW effects (LO2), LO2 with NLO QCD corrections, and LO2 with both NLO and NNLO QCD corrections. In addition, we checked that the NNLO corrections to the distributions are also stable against the cutoff  $\tau_0$ .

In Figs. 3–6, we present the charged lepton energy distribution, invariant mass distribution of the charged lepton and the hardest jet in energy in the top-quark rest frame, and two angular distributions of  $\cos(\theta^*)$  and  $\cos(\theta_{lj})$ . All of them are normalized to unit area.  $\theta^*$  are defined in the  $W$  boson rest frame as the angle between the charged lepton and the opposite of top-quark direction, and  $\theta_{lj}$  is the angle between the charged lepton and the hardest jet in the top-quark rest frame. In each figure the upper panel shows the normalized distribution while the lower panel gives their ratios with respect to that of LO1. As we can see, the differences between LO1 and LO2 are small in general, especially for the central region of each plot. Both the NLO and NNLO QCD corrections push the energy and invariant mass distributions into the central region because the recoil constituents are then massive. The NNLO corrections here are about one-fourth of the NLO ones, similar to the results of total width. Inclusive angular distribution of  $\cos(\theta^*)$  reflects the  $W$  boson helicity fractions in top-quark decay, which can be also predicted up to NNLO in QCD through top-quark self-energy calculations [24].  $\cos(\theta^*)$  distribution has been extensively studied at both the Tevatron and LHC for testing potential anomalous  $tWb$  couplings induced by new physics [7]. By a least  $\chi^2$  fit we get the  $W$  boson helicity fractions ratio as  $\mathcal{F}_L : \mathcal{F}_+ : \mathcal{F}_- = 0.689 : 0.0017 : 0.309$  using the  $\cos(\theta^*)$  distribution. The results incorporate finite  $b$  quark mass and  $W$  boson width effects, one-loop EW corrections, and QCD corrections up to NNLO, and all are in very good agreement with the one shown in Ref. [24]. Our calculations are more helpful for the corresponding measurements since experimentalists can include precise corrections for the acceptance in different kinematic regions using our results. As for  $\cos(\theta_{lj})$  distribution, QCD corrections are more pronounced there because changes of the energy spectrum also modify the distribution.

*Conclusions.*—We have presented the NNLO QCD corrections to the top-quark total decay width, which do not depend on expansion in the  $W$  boson mass, and fully differential distributions of  $t \rightarrow W^+(l^+ \nu)b$  based on SCET. One-loop EW corrections as well as effects from finite  $b$  quark mass and  $W$  boson width are also included. All together they constitute the current most precise predictions for top-quark decay, which are helpful for



top-quark mass measurement and testing of weak charged current structure. We have implemented the calculation into an efficient parton level Monte Carlo program [25], in which an arbitrary infrared-safe cut can be imposed on the final state. Our calculations are complementary to the NNLO QCD predictions for top-quark pair production [8]. Moreover, our method can be widely used in studies of heavy-to-light quark decay, including  $B$  meson semileptonic decay, which will be presented elsewhere.

We appreciate helpful discussions with P.M. Nadolsky and B. Pecjak. This work was supported by the U. S. DOE under contract DE-AC02-76SF00515, Early Career Research Award DE-SC0003870 by Lightner-Sams Foundation, and the National Natural Science Foundation of China, under Grants No. 11021092, No. 10975004 and No. 11135003.

\*jung@smu.edu

†csli@pku.edu.cn

\*hxzhu@slac.stanford.edu

- [1] M. Jezabek and J. H. Kuhn, *Nucl. Phys.* **B314**, 1 (1989); A. Czarnecki, *Phys. Lett. B* **252**, 467 (1990); C. S. Li, R. J. Oakes, and T. C. Yuan, *Phys. Rev. D* **43**, 3759 (1991).
- [2] A. Czarnecki and K. Melnikov, *Phys. Rev. D* **56**, 7216 (1997).
- [3] A. Czarnecki and K. Melnikov, *Nucl. Phys.* **B544**, 520 (1999).
- [4] K. G. Chetyrkin, R. Harlander, T. Seidensticker, and M. Steinhauser, *Phys. Rev. D* **60**, 114015 (1999).
- [5] I. R. Blokland, A. Czarnecki, M. Slusarczyk, and F. Tkachov, *Phys. Rev. Lett.* **93**, 062001 (2004).
- [6] Tevatron Electroweak Working Group, CDF, and D0 Collaborations, [arXiv:1107.5255](#); S. Blyweert (ATLAS and CMS Collaborations), [arXiv:1205.2175](#).
- [7] T. Aaltonen *et al.* (CDF and (D0 Collaborations), *Phys. Rev. D* **85**, 071106 (2012); G. Aad *et al.* (ATLAS Collaboration), *J. High Energy Phys.* **06** (2012) 088.
- [8] P. Baernreuther, M. Czakon, and A. Mitov, [arXiv:1204.5201](#).
- [9] C. Anastasiou, K. Melnikov, and F. Petriello, *Phys. Rev. Lett.* **93**, 032002 (2004); C. Anastasiou, L. J. Dixon, K. Melnikov, and F. Petriello, *Phys. Rev. D* **69**, 094008 (2004); C. Anastasiou, K. Melnikov, and F. Petriello, *Phys. Rev. Lett.* **93**, 262002 (2004); C. Anastasiou, K. Melnikov, and F. Petriello, *J. High Energy Phys.* **09** (2007) 014; A. Gehrmann-De Ridder, T. Gehrmann, E. W. N. Glover, and G. Heinrich, *Phys. Rev. Lett.* **100**, 172001 (2008); S. Weinzierl, *Phys. Rev. Lett.* **101**, 162001 (2008); S. Biswas and K. Melnikov, *J. High Energy Phys.* **02** (2010) 089; K. Melnikov, *Phys. Lett. B* **666**, 336 (2008); S. Catani, L. Cieri, G. Ferrera, D. de Florian, and M. Grazzini, *Phys. Rev. Lett.* **103**, 082001 (2009); G. Ferrera, M. Grazzini, and F. Tramontano, *Phys. Rev. Lett.* **107**, 152003 (2011); S. Catani, L. Cieri, D. de Florian, G. Ferrera, and M. Grazzini, *Phys. Rev. Lett.* **108**, 072001 (2012); C. Anastasiou, F. Herzog, and A. Lazopoulos, *J. High Energy Phys.* **03** (2012) 035; M. Czakon and A. Mitov, [arXiv:1210.6832](#).
- [10] S. Catani and M. Grazzini, *Phys. Rev. Lett.* **98**, 222002 (2007).
- [11] C. W. Bauer, S. Fleming, D. Pirjol, and I. W. Stewart, *Phys. Rev. D* **63**, 114020 (2001); C. W. Bauer, D. Pirjol, and I. W. Stewart, *Phys. Rev. D* **65**, 054022 (2002); M. Beneke, A. P. Chapovsky, M. Diehl, and T. Feldmann, *Nucl. Phys.* **B643**, 431 (2002).
- [12] G. P. Korchemsky and G. F. Sterman, *Phys. Lett. B* **340**, 96 (1994); R. Akhoury and I. Z. Rothstein, *Phys. Rev. D* **54**, 2349 (1996); C. W. Bauer and A. V. Manohar, *Phys. Rev. D* **70**, 034024 (2004); S. W. Bosch, B. O. Lange, M. Neubert, and G. Paz, *Nucl. Phys.* **B699**, 335 (2004); X. Liu, *Phys. Lett. B* **699**, 87 (2011).
- [13] R. Bonciani and A. Ferroglia, *J. High Energy Phys.* **11** (2008) 065; H. M. Asatrian, C. Greub, and B. D. Pecjak, *Phys. Rev. D* **78**, 114028 (2008); M. Beneke, T. Huber, and X.-Q. Li, *Nucl. Phys.* **B811**, 77 (2009); G. Bell, *Nucl. Phys.* **B812**, 264 (2009).
- [14] T. Becher and M. Neubert, *Phys. Lett. B* **637**, 251 (2006).
- [15] T. Becher and M. Neubert, *Phys. Lett. B* **633**, 739 (2006).
- [16] J. M. Campbell and F. Tramontano, *Nucl. Phys.* **B726**, 109 (2005).
- [17] H. Murayama, I. Watanabe, and K. Hagiwara, Report No. KEK-91-11.
- [18] K. Melnikov, A. Scharf, and M. Schulze, *Phys. Rev. D* **85**, 054002 (2012).
- [19] J. C. Collins, F. Wilczek, and A. Zee, *Phys. Rev. D* **18**, 242 (1978).
- [20] A. Denner and T. Sack, *Nucl. Phys.* **B358**, 46 (1991).
- [21] J. Beringer *et al.* (Particle Data Group Collaboration), *Phys. Rev. D* **86**, 010001 (2012).
- [22] G. Eilam, R. R. Mendel, R. Migneron, and A. Soni, *Phys. Rev. Lett.* **66**, 3105 (1991).
- [23] S. Catani, Y. L. Dokshitzer, M. Olsson, G. Turnock, and B. R. Webber, *Phys. Lett. B* **269**, 432 (1991).
- [24] A. Czarnecki, J. G. Korner, and J. H. Piclum, *Phys. Rev. D* **81**, 111503 (2010).
- [25] <http://nntopdec.hepforge.org/>.